© Indian Academy of Sciences

REVIEW

Abundances of neutron-capture elements in CH and carbon-enhanced metal-poor (CEMP) stars

MEENAKSHI PURANDARDAS* and ARUNA GOSWAMI

Indian Institute of Astrophysics, Koramangala, Bengaluru 560034, India.
*Corresponding author. E-mail: meenakshi.p@iiap.res.in

Abstract. All the elements heavier than Fe are produced either by the slow (-s) or rapid (-r) neutron-capture process. The neutron density prevailing in the stellar sites is one of the major factors that determines the type of neutron-capture processes. We present the results based on the estimates of corrected value of absolute carbon abundance, [C/N] ratio, carbon isotopic ratio and [hs/ls] ratio obtained from the high-resolution spectral analysis of six stars that include both CH stars and CEMP stars. All the stars show enhancement of neutron-capture elements. Location of these objects in the A(C) vs. [Fe/H] diagram shows that they are Group I objects, with external origin of carbon and neutron-capture elements. Low values of carbon isotopic ratios estimated for these objects may also be attributed to some external sources. As the carbon isotopic ratio is a good indicator of mixing, we have used the estimates of $^{12}C/^{13}C$ ratios to examine the occurrence of mixing in the stars. While the object HD 30443 might have experienced an extra mixing process that usually occurs after red giant branch (RGB) bump for stars with $\log(L/L_\odot) > 2.0$, the remaining objects do not show any evidence of having undergone any such mixing process. The higher values of [C/N] ratios obtained for these objects also indicate that none of these objects have experienced any strong internal mixing processes. Based on the estimated abundances of carbon and the neutron-capture elements, and the abundance ratios, we have classified the objects into different groups. While the objects HE 0110−0406, HD 30443 and CD−38 2151 are found to be CEMP-s stars, HE 0308−1612 and HD 176021 show characteristic properties of CH stars with moderate enhancement of carbon. The object CD−28 1082 with enhancement of both r- and s-process elements is found to belong to the CEMP-r/s group.

Keywords. Stars—Individual—Stars—Abundances—Stars—Carbon—Stars—Nucleosynthesis.

1. Introduction

Chemical analysis of metal-poor stars such as CH stars and CEMP stars can provide important clues about the nature of nucleosynthesis processes occurred in the early Galaxy. Especially, the abundances of neutron-capture elements can be used to constrain the Galactic chemical evolution due to heavy elements. Various sky survey programmes (HK survey and Hamburg/ESO survey, Beers *et al.* 1985; Wisotzki *et al.* 2000; Christlieb *et al.* 2001) were conducted in the past to find metal-poor stars. All these surveys show that the fraction of carbon-enhanced objects increases with decreasing metallicity (Beers & Christlieb 2005; Frebel *et al.* 2005; Norris *et al.* 2007; Spite *et al.* 2013; Yong *et al.* 2013).

CH stars are FGK giants that show strong carbon molecular bands in their spectra. They are high-radial-velocity objects, mostly found in the halo of our Galaxy. CEMP stars are the metal-poor ([Fe/H] < −1) counterparts of CH stars. Both the CH stars and CEMP stars show enhancement of carbon and neutron-capture elements. Hence, these objects are ideal candidates to study the origin and evolution of these elements. Based on the type of enhancement of neutron-capture elements, CEMP stars are classified into different groups, such as CEMP-s, CEMP-r, CEMP-r/s

and CEMP-no stars (Beers & Christlieb 2005). The evolutionary status of CH and CEMP stars do not support the enhancement of carbon and heavy elements observed in these stars. The widely accepted scenario to explain this enhancement is that these objects are in a binary system. The primary companion once passed through the Asymptotic Giant branch (AGB) phase and synthesized carbon and heavy elements. The synthesized materials are then transferred to the secondary companion through some mass transfer mechanisms. The radial velocity variations exhibited by CH and CEMP stars (McClure 1983, 1984; McClure & Woodsworth 1990; Hansen *et al.* 2016a) support this idea.

In this article, we have presented the results from the high-resolution analysis of six stars that include four CEMP stars and two CH stars. This article is organized as follows: In Section 2, we have presented a brief discussion on the new results obtained for our programme stars as some of the results from abundance analysis of these objects were presented in Purandardas *et al.* (2019), and Purandardas, Goswami & Doddamani (2019). Section 3 presents the sample selection, observations and data reductions. Section 4 describes the determination of radial velocity and stellar atmospheric parameters. Details of the abundance analysis are presented in Section 5. In Section 6, interpretation of our results are presented. Conclusions are drawn in Section 7.

2. Novelty of this work

We have presented the abundance analysis results for 26 elements in our programme stars in Purandardas *et al.* (2019), and Purandardas, Goswami & Doddamani (2019). In these works, we have also reported the mass and age of these stars as well as the results from the kinematic analysis. The location of these objects in the H-R diagram shows that they are either subgiants or in the ascending stage of the giant branch. Various mixing processes have been found to operate in giant stars. It is therefore important to understand whether the stars have undergone any internal mixing processes before interpreting the observed abundances. We had not addressed this problem in our previous works. In this article, we have checked whether any internal mixing processes have altered the surface chemical composition of these stars based on [C/N] and carbon isotopic ratios. While HD 30443 might have experienced an extra mixing process that usually occurs after red giant branch (RGB) bump for stars with log(L/

$L_\odot$) > 2.0, the remaining objects do not show any evidence of having undergone any such mixing process. In our previous works, we have not checked the possible source of enrichment of neutron-capture elements observed in our programme stars. In the present work, we have tried to understand the possible source of neutron-capture elements based on the location of the absolute carbon abundance values of the programme stars, in the A(C) vs. [Fe/H] diagram. Based on the estimated value of carbon abundances together with the observed enhancement of neutron-capture elements, we have classified them as Group I objects following the Yoon *et al.* (2016) classification scheme. As the Group I objects are all binaries, it is likely that our programme stars that belong to this group are also in binary systems with external origin of carbon and neutron-capture elements. Low values of carbon isotopic ratios estimated for these objects may also be attributed to external sources. In the present work, we have re-calculated the [hs/ls] ratio for our programme stars without considering the contribution from samarium which is an r-process element which we had taken into account for this estimation in our previous works.

3. Observations and data reduction

Programme stars are selected from the CH star catalogue of Bartkevicious (1996), Goswami (2005) and Goswami *et al.* (2010). In the latter papers, potential CH star candidates are identified based on the low-resolution (R=$\lambda/\delta\lambda$ $\sim$1330) spectroscopic studies of faint high-latitude carbon stars. In these works, two of our programme stars HE 0110−0406 and HE 0308−1612 are identified to be potential CH star candidates. We have obtained high-resolution (R $\sim$ 60,000) spectra of these objects along with HD 30443 using the high-resolution fiber-fed Hanle Echelle Spectrograph (HESP) attached to the 2 m Himalayan Chandra Telescope (HCT) at the Indian Astronomical Observatory, Hanle. The spectra cover the wavelength range from 3530 to 9970 Å. The spectrograph allows a resolution of 60,000 with slicer, and a resolution of 30,000 without slicer. The spectrum is recorded on a CCD with 4096×4096 pixels of 15 micron size. For the programme stars, CD−28 1082 and HD 176021, we have used the high-resolution FEROS spectra (Fiber-fed Extended Range Optical Spectrograph (FEROS) of 1.52 m telescope of European Southern Observatory at La Silla). The wavelength coverage of the FEROS spectra is from 3500–9000 Å with a spectral resolution

of $\sim$ 48,000. The detector is a back-illuminated CCD with 2948×4096 pixels of 15 μm size. For the object CD−38 2151, a high-resolution (R $\sim$ 72,000) spectrum was obtained using the high-resolution fiber-fed Echelle spectrometer attached to the 2.34 m Vainu Bappu Telescope (VBT) at the Vainu Bappu Observatory (VBO), Kavalur. The spectrum covers the wavelength region from 4100 to 9350 Å with gaps between orders. The spectrometer operates in two modes. It allows a resolution of 72,000 with a 60 micron slit and a resolution of 27,000 without the slit. The spectrum is recorded on a CCD with 4096×4096 pixels of 12 μm size. The data reduction is carried out using various spectroscopic reduction packages such as IRAF. Examples of a few sample spectra of the programme stars are shown in Figure 1.

4. Determination of radial velocity and stellar atmospheric parameters

Radial velocity of the programme stars were determined by measuring the shift in the wavelength for a large number of unblended and clean lines in their
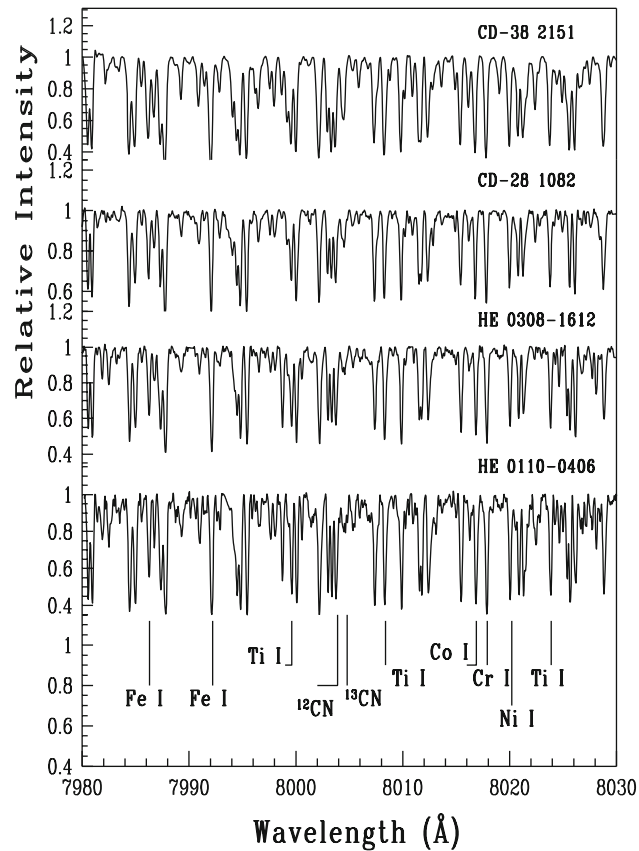

Figure 1. Sample spectra of the programme stars in the wavelength region 7980–8030 Å.

spectra. The radial velocities ranged from −26.7 to 139.7 km s^{-1}. The estimated radial velocities of the programme stars are presented in Table 1.

Stellar atmospheric parameters were determined from the measured equivalent widths of clean and unblended Fe I and Fe II lines using the local thermodynamic equilibrium (LTE) analysis. We made use of the recent version of MOOG of Sneden (1973) for our analysis. Model atmospheres were selected from Kurucz grid of model atmospheres with no convective overshooting (http://cfaku5.cfa.hardvard.edu/). Solar abundances were taken from Asplund *et al.* (2009). The effective temperature was taken to be that value for which the trend between the abundance derived from Fe I lines and the corresponding excitation potential gives a zero slope. At this temperature, the microturbulent velocity was determined for which the abundance derived from Fe I lines do not exhibit any dependence on the reduced equivalent width. Corresponding to these values of effective temperature and microturbulent velocity, log *g* was determined in such a way that the abundances obtained from Fe I and Fe II lines were nearly the same. Only those lines with excitation potential from 0.0–5.0 eV and equivalent widths from 20–180 mÅ were considered for the analysis. The derived atmospheric parameters and the radial velocities are listed in Table 1.

5. Abundance analysis

The detailed discussion on the abundance analysis results for the six programme stars are presented in Purandardas *et al.* (2019), and Purandardas, Goswami & Doddamani (2019). Here we present a brief summary of these results. However, here we give greater emphasize to the results based on the absolute carbon abundance, [C/N] ratio, carbon isotopic ratio and the [hs/ls] ratio which is recalculated in this work.

The abundances of various elements were determined from the measured equivalent widths of absorption lines due to neutral and ionized elements. We have used only the symmetric and clean lines for our analysis. Lines were identified by plotting the arcturus spectra upon the individual spectra of our programme stars. Then a master line list was prepared using the measured equivalent widths and other line information such as lower excitation potential and the loggf values taken from the Kurucz database. We have also consulted the VALD database. We could estimate the abundances of 24 elements which include the light elements C, N, O, odd-Z element Na, α- and Fe-peak

Table 1. Derived atmospheric parameters and radial velocities of the programme stars.

Star	T_{eff} (K)	log g (cgs)	ζ (km s^{-1})	[Fe I/H]	[Fe II/H]	V_r (km s^{-1})
HE 0110−0406	4670	1.00	1.92	−1.31 ± 0.09	−1.29 ± 0.12	−44.40 ± 3.8 (HESP)
HE 0308−1612	4600	1.70	1.42	−0.72 ± 0.19	−0.73 ± 0.15	85.5 ± 1.22 (HESP)
CD−28 1082	5200	1.90	1.42	−2.46 ± 0.08	−2.44 ± 0.02	−26.7 ± 0.3 (FEROS)
HD 30443	4040	2.05	2.70	−1.68 ± 0.05	−1.69 ± 0.11	66.61 ± 0.20 (HESP)
CD−38 2151	4600	0.90	2.30	−2.03 ± 0.10	−2.03	139.7 ± 1.9 (VBT)
HD 176021	5900	3.95	1.02	−0.62 ± 0.08	−0.65 ± 0.05	109.1 ± 0.5 (FEROS)

elements Mg, Si, Ca, Ti, V, Cr, Mn, Co, Ni and Zn and the neutron-capture elements Sr, Y, Zr, Ba, La, Ce, Pr, Nd, Sm and Eu. We have also used spectrum synthesis calculations for elements such as Sc, V, Mn, Ba, La and Eu taking their hyperfine structures into considerations. The hyperfine structures of Sc, V and Mn were taken from Prochaska & McWilliam (2000). For Ba, La and Eu, the hyperfine structures were taken from McWilliiam (1998), Jonsell *et al.* (2006) and Worley *et al.* (2013) respectively.

We could estimate oxygen abundance only for CD−38 2151 and HD 30443. For these objects, the abundance of oxygen was determined from the spectrum synthesis calculations of the [OI] line at 6300.3 and OI line at 6363.8 Å. The carbon abundance could be determined for all the objects from the spectrum synthesis calculations of the C_2 molecular band at 5165 Å. We could estimate the carbon isotopic ratio for all of our programme stars except HD 176021 using the spectrum synthesis calculation of CN band at 8005 Å (Figure 2). The values lie in the range from 7.4 to 45. Abundance of nitrogen was estimated using the spectrum synthesis calculation of CN band at 4215 Å. Nitrogen was found to be enhanced in CD−28 1082 and CD−38 2151. Other objects exhibit moderate enhancement in nitrogen. The molecular lines for C_2 and CN were taken from Brooke *et al.* (2013), Sneden *et al.* (2014) and Ram *et al.* (2014). The estimated values of carbon and nitrogen are presented in Table 2.

Sodium was moderately enhanced in all our programme stars except HD 176021 in which Na is near solar. HE 0110−0406 and HD 176021 show near solar abundances of alpha elements, while HE 0308−1612 shows slight enhancement of these elements. We could not estimate Si in these objects. Among the alpha elements, we could estimate only Mg and Ca in CD−28 1082 with [Mg/Fe] ∼ 0.45 and [Ca/Fe] ∼ 0.27. In HD 30443, Si and Ca were moderately enhanced with [Si/Fe] ∼ 0.82 and [Ca/Fe] ∼ 0.51, while magnesium, Sc and Ti are near solar abundance.

Magnesium and Ca are found to be moderately enhanced in CD−38 2151, while Si was found to be enhanced with [Si/Fe] ∼ 1.62. Scandium and Ti are found to be near solar abundance in this object.

HE 0110−0406 shows near solar abundance of Fe peak elements except Ni which is slightly enhanced with [Ni/Fe] ∼ 0.45. While Fe-peak elements were slightly enhanced in HE 0308−1612. We could not estimate Co in HE 0308−1612. Among the Fe peak elements, we could estimate only Mn in CD−28 1082, which was found to be enhanced with [Mn/Fe] ∼ 1.48. In HD 30443, Mn and Co were near solar abundance and Ni is moderately enhanced with [Ni/Fe] ∼ 0.59. Cobalt and Ni are near solar abundance in CD−38 2151. While chromium is slightly enhanced and Mn is under-abundant with [Mn/Fe] ∼ −0.20. In HD 176021, all the Fe peak elements are found to be near solar abundance.

All of our programme stars exhibit enhancement of neutron-capture elements. From our detailed analysis, we found that CD−28 1082 is a CEMP-r/s star and the objects HE 0110−0406, CD−38 2151 and HD 30443 are CEMP-s stars. We could not estimate Eu in HD 30443 and CD−38 2151. Hence, it is not possible to classify these stars based on the criteria as given by Beers & Christlieb (2005). In this case, we have used the criteria for the classification of CEMP-s stars as given by Hansen *et al.* (2019) based on [Sr/Ba] ratio. According to this classification scheme, [Sr/Ba] > −0.5 can be used to separate CEMP-s stars from CEMP-r/s stars. HD 30443 and CD−38 2151 show [Sr/Ba] ∼ −0.27 and [Sr/Ba] ∼ 0.88 respectively. HE 0308−1612 and HD 176021 exhibit the properties of CH subgiants. All the programme stars showed enhancement of heavy *s*-process elements more than the light *s*-process elements except for CD−38 2151 and HD 176021. The abundance results for neutron-capture elements are listed in Table 3. In this table, ls stands for light *s*-process elements (Sr, Y and Zr) and hs represents the heavy *s*-process elements (Ba, La, Ce, and Nd).
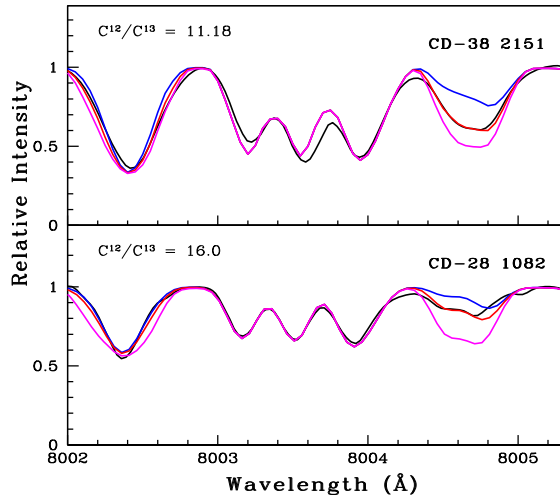
Figure 2. Synthesis of CN band around 8005 Å. Synthesized spectra is shown in red colour and the observed spectra is represented in black colour. Synthetic spectra corresponding to $^{12}C/^{13}C \simeq 12$ (blue) and 1 (magenta) are also shown.

6. Interpretation of results

The interpretation of the results based on the corrected value of absolute carbon abundance, [C/N], carbon isotopic ratios and [hs/ls] ratios obtained for our programme stars are presented here in detail. Understanding the possible source of origin of the enhancement of neutron-capture elements is very important to understand the type of nucleosynthesis process which produced it. One of the best ways to get any clues regarding the source is to locate the stars in the A(C) vs. [Fe/H] diagram. It is found that CEMP stars exhibit a bimodal distribution in the A(C) vs. [Fe/H] diagram. Spite *et al.* (2013) claims the occurrence of two plateau at A(C) = 8.25 and another at A(C) = 6.50. While Yoon *et al.* (2016) confirmed two peaks at A(C) = 7.96 and A(C) = 6.28,

Table 3. Ratios of light and heavy *s*-process elements.

Star	[Fe/H]	[ls/Fe]	[hs/Fe]	[hs/ls]
HE 0110−0406	−1.30	1.03	1.36	0.33
HE 0308−1612	−0.73	1.11	1.62	0.51
CD−28 1082	−2.45	1.52	1.90	0.38
HD 30443	−1.69	1.24	1.93	0.69
CD−38 2151	−2.03	1.24	1.10	−0.14
HD 176021	−0.64	1.50	1.37	−0.13

respectively, for high- and low-carbon regions corresponding to the corrected carbon values. The stars that occupy the high-carbon region are mostly found to be in binary systems. Hence, the observed enhancement of carbon is attributed to the binary companion. Stars that occupy the low-carbon region are found to be single and the observed carbon abundance is intrinsic in origin. CEMP stars are classified by Yoon *et al.* (2016) into three groups based on the morphology in the A(C) vs. [Fe/H] diagram. Group I objects are mainly composed of CEMP-s and CEMP-r/s stars. These objects show a weak dependence of A(C) on [Fe/H]. The absolute carbon abundance, A(C) of Group II objects, shows a clear dependence on [Fe/H]. While for Group III objects, A(C) is found to be independent of [Fe/H], Group II and Group III objects are mainly composed of CEMP-no stars. In Figure 3, the location of our programme stars are shown in the A(C) vs. [Fe/H] diagram. We have applied corrections to the estimated carbon abundances using the public online tool by Placco *et al.* (2014) available at http://vplacco. pythonanywhere.com/. The corrected carbon values are listed in Table 2. Figure 3 shows that all of our programme stars are Group I objects. Hence, we assumed that the observed enhancement of carbon may be attributed to the binary companion.

Table 2. Abundance results for carbon, nitrogen, C/O and carbon isotopic ratios.

Star	$\log \epsilon$ (C)	$\log \epsilon$ (C)*	[C/Fe]	$\log \epsilon$ (N)	[N/Fe]	C/O	$^{12}C/^{13}C$
HE 0110−0406	7.85	7.98	0.73	7.15	0.63	–	45.0
HE 0308−1612	8.48	8.50	0.78	7.25	0.15	–	15.6
CD−28 1082	8.16	8.23	2.19	8.10	2.73	–	16.0
HD 30443	8.43	8.47	1.68	6.55	0.40	1.02	7.40
CD−38 2151	7.90	8.02	1.50	7.20	1.40	2.95	11.2
HD 176021	8.33	8.33	0.52	7.80	0.59	–	–

* Corrected value of carbon.

The low values of $^{12}C/^{13}C$ ratio observed in our programme stars also support the extrinsic origin of carbon. Various mixing processes, such as first dredge up (FDU), thermohaline mixing and rotation-induced mixing (Charbonnel 2005; Dearborn *et al.* 2006; Eggleton *et al.* 2006), can cause a low carbon isotopic ratio. Vanture (1992) suggests that certain nucleosynthetic reactions of the accreted material can reduce the ^{12}C abundance. We have estimated the [C/N] ratio of our programme stars to derive any clues to know if they have undergone any mixing processes. Since nitrogen is produced at the expense of carbon, the [C/N] ratio acts as a sensitive indicator of mixing. Spite *et al.* (2005) analysed CNO and Li abundances for a sample of extremely metal-poor stars. Their analysis shows that the stars that exhibit clear evidence of mixing have a low value of [C/N] ratio (< −0.60), and they belong to upper RGB or horizontal branch. The stars that do not show any evidence of mixing have [C/N] > −0.60 and lie on the lower RGB. Figure 4 shows that all of our programme stars have [C/N] > −0.6. This implies that none of our programme stars have undergone any significant internal mixing processes.
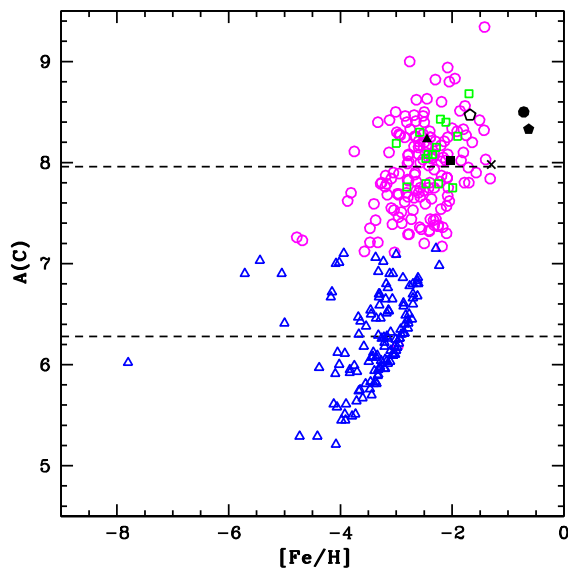

Figure 3. Corrected A(C) vs. [Fe/H] diagram for the compilation of CEMP stars taken from Yoon *et al.* (2016). CEMP-s stars are represented by open circles. CEMP-r/s and CEMP-no stars are shown by open squares and open triangles respectively. Programme stars are represented by black coloured symbols, HE 0110−0406 (cross), HE 0308−1612 (filled circle), CD−28 1082 (filled triangle), HD 30443 (open pentagon), CD−38 2151 (filled square) and HD 17602 (filled pentagon).

Stellar models predict that when a low-mass star ascends the Red Giant Branch, the outer convective envelope expands inwards and penetrates into the region of CN processed materials (FDU). The luminosity at which the FDU occurs in low-mass field stars is $\log(L/L_\odot) \sim 0.80$ (Gratton *et al.* 2000). All of our programme stars have $\log(L/L_\odot) > 0.80$, except HD 176021. Hence, they might have undergone FDU. However, these stars fall in the unmixed category. Although, in solar mass/metallicity stars, the $^{12}C/^{13}C$ ratio decreases by a factor of 20–30 from the original value and surface abundance of nitrogen increases after FDU (Iben & Renzini 1984), it is found to be less efficient in metal-poor stars (VandenBerg & Smith 1988, Charbonnel 1994). This implies that the changes in the surface compositions of C and N after the occurrence of FDU are very small in metal-poor stars. The carbon abundance is found to be decreased only by about 0.05 dex and the decrease in the $^{12}C/^{13}C$ ratio is not large enough for these stars (Gratton *et al.* 2000).

A second mixing episode can happen when the star becomes brighter than the RGB bump at a luminosity of $\log(L/L_\odot) \sim 2.0$. In this process, ^{12}C abundance decreases by a factor of ~ 2.5 and $^{12}C/^{13}C$ reaches a value of ~ 6 to 10. Nitrogen abundance also increases by a factor of nearly 4 (Gratton *et al.* 2000). Two of our programme stars, HD 30443 and CD−38 2151, have $\log(L/L_\odot) \sim 2.2$ and 2.87, respectively. Hence, they are expected to show the signatures of mixing. But these stars show no signatures of mixing based on [C/N] ratio. Spite *et al.* (2006) suggest that [C/N] ratio is not a clean indicator of mixing as the abundance of C and N in the interstellar medium from which these stars are formed show large variations. In that case, one can use the $^{12}C/^{13}C$ as a good indicator of mixing, since it is high in primordial matter (> 70) and the determination of carbon isotopic ratio is found to be insensitive to the choice of atmospheric parameters for the stars (Spite *et al.* 2006). We have plotted $^{12}C/^{13}C$ ratio and T_{eff} of our programme stars as shown in Figure 5. From the figure, it is clear that the object HD 30443 share the region occupied by the stars that have undergone internal mixing processes. This means that HD 30443 had experienced internal mixing processes that might have altered its initial surface chemical compositions. CD−38 2151 lies close to the boundary of separation of mixed and unmixed stars. The low value of carbon isotopic ratio in other programme stars may be interpreted as the result of strong processing in the
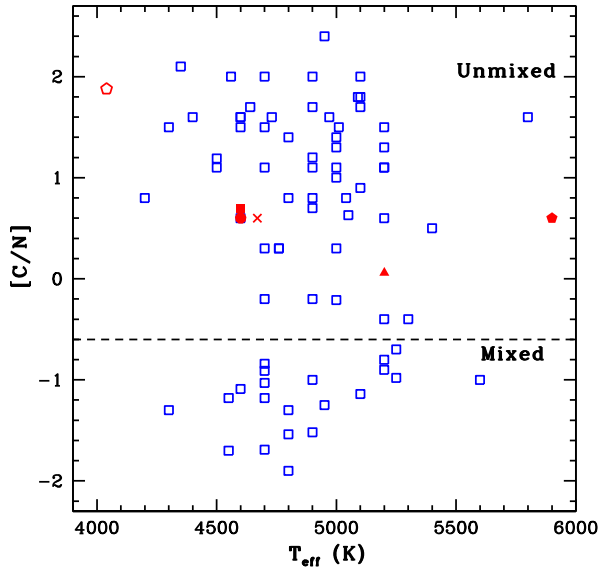
Figure 4. Position of the programme stars in the [C/N] vs. T_{eff} diagram. Programme stars are represented using red coloured symbols. The symbols used for the programme stars are same as in Figure 3. Open squares represent the stars from literature (Spite *et al.* 2006; Aoki *et al.* 2007; Goswami *et al.* 2016; Hansen *et al.* 2016b, 2019).
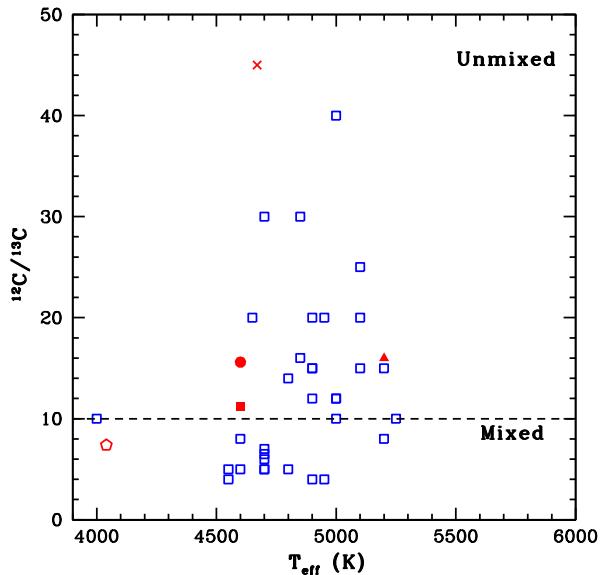

Figure 5. Position of the programme stars in $^{12}C/^{13}C$ vs. T_{eff} diagram. Programme stars are represented using red coloured symbols. The symbols used for the programme stars are same as in Figure 3. Open squares represent the stars from Spite *et al.* (2006) and Aoki *et al.* (2007).

AGB progenitors (Hansen *et al.* 2016b) and not in the star itself.

From the estimated carbon isotopic ratio and the location of our programme stars in the A(C) vs. [Fe/H]

diagram, we assume that the observed enhancement of neutron-capture elements may be attributed to an extrinsic source. As Group I objects are mostly found to be associated with binary systems, the enhancement may be justified by the mass transfer from the binary companion.

According to Busso *et al.* (2001), the light s-process elements such as Y, Zr and Sr are predominantly produced in AGB stars with near solar metallicity. Hence, mass transfer from such a companion can produce more enhancement of light s-process elements than the heavy s-process elements. The AGB stars with [Fe/H] ~ -1.0 can produce more heavy s-process elements such as Ba, La, Ce and Nd than the light s-process elements, and this leads to lower [ls/Fe] than [hs/Fe] in the stars that have accreted materials from the metal-poor AGB stars. The reason is that, in the metal-poor AGB stars, the number of Fe seed nuclei available for neutron-capture process is less and hence the neutron exposure for each Fe seed nuclei will be more. This leads to the formation of more heavier elements. The binary mass transfer scenario can similarly be applied to justify the observed enhancement of neutron-capture elements in CD-28 1082 which is a CEMP-r/s star. Several authors (Hampel *et al.* 2016; Hansen *et al.* 2016a and references therein) have shown that the observed abundance patterns of CEMP-r/s stars are consistent with the model calculations of i-process in low-metalicity AGB stars.

7. Conclusion

The possible source of the origin of enhancement of neutron-capture elements in six carbon stars were examined in the light of absolute carbon abundances. The location of our programme stars in the A(C) vs. [Fe/H] diagram shows that these objects belong to Group I category. Various studies on radial velocities of these objects show that most of them exhibit radial velocity variations. That is, these objects are mostly found to be associated with binary systems. Hence, the observed enhancement of carbon and neutron-capture elements in our programme stars may be attributed to the binary companion. But none of the programme stars are known to be confirmed binaries. The low values of carbon isotopic ratio also supports the extrinsic origin.

Elemental abundance ratios also bear important signatures about the source of enrichment of neutron-capture elements. We have re-estimated the [hs/ls]

ratio for our programme stars. Abate *et al.* (2015) predict an [ls/hs] ratio less than zero for AGB models. All the programme stars except CD−38 2151 and HD 176021 show an [hs/ls] ratio characteristics of AGB progenitors.

We have also examined whether the programme stars have undergone any internal mixing based on [C/N] and carbon isotopic ratios. It is important to understand whether the mixing have modified the surface composition of the star before interpreting the observed abundance patterns. We found that none of the programme stars have experienced internal mixing, except HD 30443. The estimated values of [C/N] ratio also show that the objects have not gone through any significant mixing processes. Thus, the observed values of low carbon isotopic ratio in the unmixed stars may be due to the strong mixing processes occurred in the AGB progenitors. In other words, the observed surface chemical compositions of our programme stars, except HD 30443, preserve the fossil records of the materials synthesised in the AGB stars from which they have accreted the materials.

Acknowledgements

References

Abate C., Pols O.R., Izzard R.G., Karakas A.I., 2015, A&A, 581, A22

Aoki W., Beers T.C., Christlieb N., Norris J.E., Ryan S.G *et al.*, 2007, ApJ, 655, 492

Asplund M., Grevesse N., Sauval A.J., 2009, Ann. Rev. Astron. Astrophy., 47, 481

Bartkevicious A., 1996, Baltic Astron, 5, 217

Beers T.C., Preston G.W., Shectman S.A., 1985, AJ, 90, 2089

Beers T.C., Christlieb N., 2005, ARA&A, 43, 531

Brooke J.S., Bernath P.F., Schmidt T.W., Bacskay G.B., 2013, J.Quant. Spectrosc. Radiat. Transfer, 124, 11

Busso M., Gallino R., Lambert D.L., Travaglio C., Smith V.V., 2001, ApJ, 557, 802

Charbonnel C., 2005, ASP Conference Series, Vol. 336

Christlieb N., Green P. J., Wisotzki L., Reimers D., 2001, A&A, 375, 366

Dearborn D. S. P., Lattanzio J. C., Eggleton P. P., 2006, ApJ, 639, 405

Eggleton P. P., Dearborn D. S. P., Lattanzio J. C., 2006, Science, 314, 1580

Frebel A., Aoki W., Christlieb N., Ando H., Asplund M. *et al.*, 2005, Nature, 434, 871

Goswami A., 2005, MNRAS, 359, 531

Goswami A., Karinkuzhi D., Shantikumar N.S., 2010, MNRAS, 402, 1111

Goswami A., Aoki W., Karinkuzhi D., 2016, MNRAS, 455, 402

Gratton R., Sneden C., Carretta E., Bragaglia A., 2000, A&A, 354, 169

Hampel M., Stancliffe R.J., Lugaro M., Meyer B.S., 2016, ApJ, 831, 171

Hansen C.J., Nordström B., Hansen T.T., Kennedy C.R., Placco V M. *et al.*, 2016b, A&A, 588, A37

Hansen T. T., Andersen J., Nordström B., Beers T.C., Placco V.M. *et al.* 2016a, A&A, 586, A160

Hansen C.J., Hansen T.T., Koch A., Beers T.C., Nordström B. *et al.*, 2019, A&A, 623, 128

Iben I.Jr., Renzini A., 1984, Phys. Letters 105, 329

Jonsell K., Barklem P.S., Gustafsson B., Christlieb N., Hill V. *et al.*, 2006, A&A, 451, 651

McClure R.D., 1983, ApJ, 208, 264

McClure R.D., 1984, ApJ, 280, 31

McClure R.D., Woodsworth W., 1990, ApJ, 352, 709

McWilliiam A., 1998, AJ, 115, 1640

Norris J.E., Christlieb N., Korn A.J., Eriksson K., Bessell M.S. *et al.*, 2007, ApJ, 670, 774

Placco V.M., Frebel A., Beers T. C., Stancliffe R. J., 2014, ApJ, 797, 21

Prochaska J.X., McWilliam A. 2000, ApJ, 537, 57

Purandardas M., Goswami A., Goswami P.P., Shejeelammal J., Masseron T., MNRAS, 2019, 486,3266

Purandardas M., Goswami A., Doddamani V.H., 2019, BSRSL, 88, 207

Ram R.S., Brooke James S.A., Bernath P.F., Sneden C., Lucatello S., 2014, ApJS, 211, 5

Sneden C., 1973, PhD thesis, Univ. Texas

Sneden C., Lucatello S., Ram R.S., Brook J.S.A., Bernath P., 2014, Ap. J. Supp., 214, 26

Spite M., Cayrel R., Plez B., Hill V., Spite F. *et al.*, 2005, A&A 430, 655

Spite M., Cayrel R., Hill V, Spite F., Francois P. *et al.*, 2006, A&A 455, 291

Spite, M., Caffau, E., Bonifacio, P., Spite F., Ludwig H.-G. *et al.* 2013, A&A, 552, 107

VandenBerg D.A., Smith G.H., 1988, PASP 100, 314

Yong D., Norris J. E., Bessell M. S., Christlieb N., Asplund M. *et al.*, 2013, ApJ, 762, 26

Yoon J., Beers T.C., Placco V.M., Rasmussen K.C., Carollo D. *et al.*, 2016, ApJ, 833, 20

Vanture A.D., 1992, AJ, 104, 1977

Wisotzki L., Christlieb N., Bade N., Beckmann V., Köhler T, *et al.*, 2000, A&A, 358, 77

Worley C.C., Hill V.J., Sobeck J., Carretta E., 2013, A&A, 553, A47